Table 3

Setup	Geometric origin K_1	Geometric origin C_1	Kinematic origin K_2	Kinematic origin C_2	Measured turbulence intensity,[a] % 1	2	3
Screen and filter	0.130	−15.0	0.227	2.00	1.06	0.975	2.81
Filter only	0.127	−5.00	0.222	0	1.28	1.45	3.66
Filter and rods	0.113	−6.00	0.194	−1.00	1.21	1.45	2.82

[a] 1 Turbulence at mouth of jet; 2 Turbulence ½ in. upstream from mouth of jet; 3 Turbulence ¾ in. upstream from mouth of jet.

Having discarded the possibility that the shape of the contracting nozzle could influence the location of the origins a second test was run to determine whether upstream conditions capable of changing the stream turbulence had a considerable effect.

In this second test, a different 25 in. × 25 in. plenum chamber was used. The slot was 1 in. wide by 25 in. high. The slot ended in a wall extending 24 in. from either side of it. The resulting two-dimensional jet was confined between two horizontal plywood sheets now extending 96 in. downstream and 24 in. to each side, similar to the earlier test. The Reynolds number of the flow from the orifice based on the slot's width ranged from 2.3×10^4 to 2.55×10^4. The plenum chamber was similar to that of the first run except for the fact that the wire screening was removable and could be replaced by a series of ¼ in. square rods, 2 in. on center. This was purposely done to provide three different configurations giving different turbulence intensities upstream of the slot. The results are shown in Table 3.

In the aforementioned, the obvious observation is that the location of the virtual origins can be drastically changed by affecting plenum chamber conditions. There appears to also be a slight decrease in the widening and decay rates with upstream turbulence. The tabulated measurements of turbulence intensity were crude spot checks taken only at the center of the jet. The configurations suggest that a slight increase of turbulence upstream of the contraction may move the virtual origins considerably upstream. This may be explained by the enhanced mixing. At the same time these appear to be independent of nozzle shape, plenum chamber width and slot width, and what is of even greater interest they do not tend to coincide in their locations. This lack of coincidence in location of the two virtual origins and their seemingly strong dependence on stream turbulence intensity casts a new light into the usual concept of a unique origin of similarity in turbulent freejets.

References

[1] Abramovich, G. N., *The Theory of Turbulent Jets*, The M.I.T. Press, Cambridge, Mass., 1963.

[2] Albertson, M. J. et al., "Diffusion of Submerged Jets," *Proceedings of the American Society of Chemical Engineers*, Vol. 74, Dec. 1948, pp. 1571–1596.

[3] Miller, D. R. and Comings, E. W., "Static Pressure Distribution in the Free Turbulent Jet," *Journal of Fluid Mechanics*, Vol. 3, No. 1, Oct. 1957, pp. 1–16.

[4] Sato, H., "The Stability and Transition of a Two-Dimensional Jet," *Journal of Fluid Mechanics*, Vol. 7, No. 5, 1959, pp. 53–80.

[5] Foss, J. F., "A Study of Incompressible Bounded Turbulent Jets," Ph.D. thesis, Jan. 1965, Purdue Univ.

[6] Goldschmidt, V. W., "Two-Phase Flow in a Two-Dimensional Turbulent Jet," dissertation, Jan. 1965, Syracuse Univ.

[7] Heskestad, G., "Hot-Wire Measurements in a Plane Turbulent Jet," *Transactions of the ASME, Journal of Applied Mechanics*, Dec. 1965, pp. 721–734.

[8] Householder, M. K. and Goldschmidt, V. W., "Turbulent Diffusion of Small Particles in a Two-Dimensional Free Jet," TR FMTR 68-3, 1968, National Science Foundation.

[9] Van der Hegge Zijnen, B. G., "Measurements of the Velocity Distribution in a Plane Turbulent Jet of Air," *Applied Scientific Research*, Vol. 7, Sec. A, 1957, pp. 256–276.

Buckling of Clamped and Simply Supported Shallow Spherical Shells

GERALD A. COHEN*

Structures Research Associates, Newport Beach, Calif.

IN Ref. 1, Stein has compared the theoretical buckling pressures for shallow spherical shells with clamped (Refs. 2 and 3) and simply supported edges (Ref. 3). He states that a paradox exists for $3 < \lambda < 5$, where λ is the usual shallow spherical shell parameter $2[3(1 - \nu^2)]^{1/4}(H/t)^{1/2}$, since in this region the buckling pressure for clamped edges is apparently below that for simply supported edges. He also suggests the possibility that in this region the $N = 1$ buckling mode (which was not studied in Ref. 3) may be critical for simply supported edges, and that the associated critical pressure may be below the clamped shell buckling pressure.

These statements are no doubt based on the assumption that the introduction of additional edge constraint increases the buckling load, which, of course, is the case for most structures. This assumption is, in fact, based on the energy method of solution, in which the buckling load is usually expressed as the minimum value of a certain functional of kinematically admissible displacement fields. Since the introduction of additional edge constraint reduces the family of admissible displacements, it also must raise (at least, not lower) the associated minimum value, i.e., the buckling load. However, it is frequently overlooked that this functional, by virtue of its dependence on the prebuckling state, also changes with the introduction of additional edge constraint. Insofar as this occurs, the aforementioned argument breaks down and additional edge constraint can, in fact, reduce the buckling load (as indeed it does when a shallow segment is cut from a complete spherical shell and its edges are clamped). Therefore, no paradox really exists. On the other hand, the $N = 1$ mode should be investigated for simply supported edges, and to assess its importance a brief study, using computer programs based on the analyses presented in Refs. 4 and 5, was made and is reported here.

For this purpose, a 20° spherical cap with $t/R = 0.02462$ and $\nu = \frac{1}{3}$, corresponding to $\lambda = 4$, loaded by a uniform normal pressure field was considered. For this shell, the classical buckling pressure p_{cl} is given by $p_{cl}/E \times 10^5 = 74.24$. The dimensionless prebuckling stiffness KR^3/E and its derivative with respect to the dimensionless pressure p/E were computed for four values of p/p_{cl} for simply supported edges and two values of p/p_{cl} for clamped edges. These results are shown in Table 1. The results given in Table 1 are plotted in Fig. 1, in which the curves have been extrapolated to zero stiffness, corresponding to the limit load pressure p_0. As shown, for clamped edges $p_0/p_{cl} = 0.583$, which agrees well with the value 0.578 given in Ref. 2. As expected from the results of Ref. 3, removing the rotational edge constraint increases the limit load. The value obtained, $p_0/p_{cl} = 0.710$, is, however, significantly greater than the value 0.65 given in Ref. 3.

Table 1 Stiffness variation of shallow spherical shells ($\lambda = 4$)

p/p_{cl}	$p/E \times 10^5$	Simply supported KR^3/E	Simply supported $d(KR^3)/dp$	Clamped KR^3/E	Clamped $d(KR^3)/dp$
0.5	37.12	0.1212	−374	0.1323	−896
0.578	42.91	...	...	0.0372	−4404
0.6	44.54	0.0897	−495	...	...
0.65	48.26	0.0684	−698	...	...
0.7	51.97	0.0258	−2247	...	...

Received June 9, 1969; revision received August 19, 1969.

* President and Technical Director. Member AIAA.

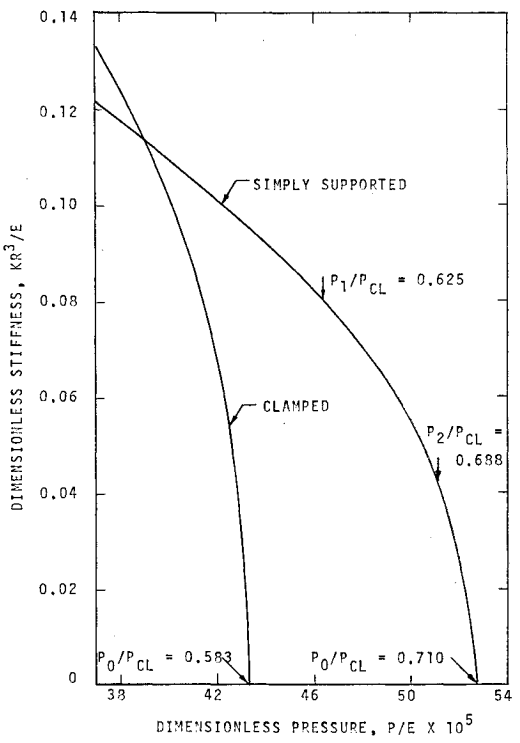

Fig. 1 Stiffness variation of shallow spherical shells ($\lambda = 4$) under uniform live pressure.

In addition to the above calculations, the $N = 1$ and $N = 2$ bifurcation pressures were computed for simply supported edges. In these calculations, linearization of the prebuckling state was made about the nonlinear prebuckling states corresponding to $p/p_{c1} = 0.60$ and 0.65 for the $N = 1$ and 2 buckling modes, respectively. As indicated in Fig. 1, the bifurcation pressures are $p_1/p_{c1} = 0.625$ and $p_2/p_{c1} = 0.688$. These compare with the $N = 2$ result of $p_2/p_{c1} = 0.65$ given in Ref. 3. Thus, as Stein suspected, the $N = 1$ buckling mode is critical for simply supported edges, but the associated critical pressure is still above the clamped shell buckling pressure.

In order to assess the effect of small geometric imperfections on these two buckling modes, the associated values of the second post-buckling coefficient b and the first imperfection parameter α were also computed. Based on buckling modes normalized to have their maximum normal deflection equal to the shell thickness, $b = -1.54$ for the $N = 1$ mode and $b = -1.06$ for the $N = 2$ mode. Also, for imperfections in the shape of the buckling modes, $\alpha = 0.581$ for the $N = 1$ mode and $\alpha = 0.386$ for the $N = 2$ mode. From these results and Eq. (78) of Ref. 5, it is clear that the $N = 1$ mode not only has a lower bifurcation pressure but is also more sensitive to small imperfections than the $N = 2$ mode. As an example, for an imperfection with a normal deflection amplitude of only one-tenth of the shell thickness, Eq. (38) of Ref. 5 gives a buckling load knockdown factor for the $N = 1$ mode of 0.672. Thus, for this very small imperfection, the shell would snap at a pressure of only 42% of the classical value for the complete spherical shell. It is interesting to note that this value is in rather good agreement with the experimental results shown for $\lambda = 4$ in Ref. 1 and 2.

References

[1] Stein, M., "Some Recent Advances in the Investigation of Shell Buckling," *AIAA Journal*, Vol. 6, No. 12, Dec. 1968, pp. 2339–2345.

[2] Huang, N. C., "Unsymmetric Buckling of Thin Shallow Spherical Shells," *Journal of Applied Mechanics*, Vol. 31, 1964, pp. 447–457.

[3] Weinitschke, H. L., "Asymmetric Buckling of Shallow Spherical Shells," *Journal of Mathematis and Physics*, Vol. 44, June 1965, pp. 141–163.

[4] Cohen, G. A., "Computer Analysis of Asymmetric Buckling of Ring-Stiffened Orthotropic Shells of Revolution," *AIAA Journal*, Vol. 6, No. 1, Jan. 1968, pp. 141–149.

[5] Cohen, G. A., "Effect of a Nonlinear Prebuckling State on the Postbuckling Behavior and Imperfection Sensitivity of Elastic Structures," *AIAA Journal*, Vol. 6, No. 8, Aug. 1968, pp. 1616–1619; also "Reply by Author to J. R. Fitch and J. W. Hutchinson," *AIAA Journal*, Vol. 7, No. 7, July 1969, pp 1407–1408.

Effect of Real Gas Properties on the Base Pressure of a Blunt-Nosed Vehicle

WENDELL NORMAN*
ARO Inc., Arnold Air Force Station, Tenn.

THE purpose of this Note is to point out the possibility that the base pressure of a blunt-nosed vehicle flying through the atmosphere at high velocities may be influenced by real gas properties. The values of base pressure in flight should be higher than those obtained in cold flow wind tunnels, which are essentially perfect gas facilities. The effect should be large for blunt vehicles and small for sharp-nosed slender vehicles.

In order to illustrate the possible differences, the hypothetical blunt-nosed vehicle shape shown in Fig. 1 is assumed. This particular shape was chosen to accentuate the real gas effects. The re-entry trajectory of Fig. 1 was taken from Ref. 1. The conditions are such that one may assume a turbulent boundary layer and, as a consequence, a negligible variation of base pressure with Reynolds number. The conditions of the gas on the flare (F) can be obtained using the following assumptions: 1) the flare pressure ratio, P_F/P_S is the same in flight as in the tunnel, and 2) the entropy increase across the flare shock is negligible.

The assumed variation of flare pressure ratio with free-stream Mach number is given in the lower part of Fig. 2.

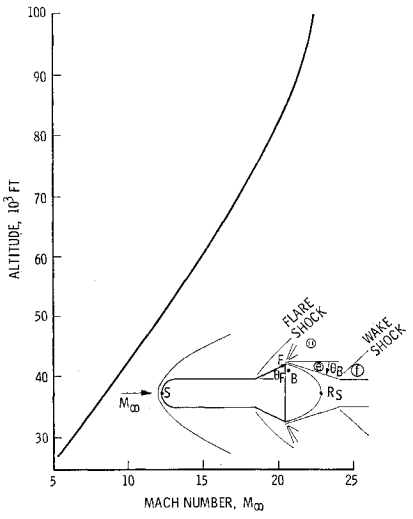

Fig. 1 Assumed model and trajectory.

Received June 13, 1969. The work reported herein was supported by the Arnold Engineering Development Center, Air Force Systems Command, under Contract F40600-69-C-0001 with ARO Inc. Further reproduction is authorized to satisfy the needs of the U.S. Government.

* Manager, Hypervelocity Branch, von Kármán GasDynamics Facility. Member AIAA.